EDITOR'S NOTE: *This study was made possible through a research grant from the AAID Research Foundation.*

IMPLANT BIOMECHANICS IN GRAFTED SINUS: A FINITE ELEMENT ANALYSIS

Mete I. Fanuscu, DDS
Hung V. Vu, DDS, PhD
Bernard Poncelet, MS

KEY WORDS

Implant
Stress
Posterior maxilla
Sinus graft
Bone stiffness

This in vitro study investigated the stress distribution in the bone surrounding an implant that is placed in a posterior edentulous maxilla with a sinus graft. The standard threaded implant and anatomy of the crestal cortical bone, cancellous bone, sinus floor cortical bone, and grafted bone were represented in the 3-dimensional finite element models. The thickness of the crestal cortical bone and stiffness of the graft were varied in the models to simulate different clinical scenarios, representing variation in the anatomy and graft quality. Axial and lateral loads were considered and the stresses developed in the supporting structures were analyzed. The finite element models showed different stress patterns associated with helical threads. The von Mises stress distribution indicated that stress was maximal around the top of the implant with varying intensities in both loading cases. The stress was highest in the cortical bone, lower in the grafted bone, and lowest in the cancellous bone. When the stiffness of the grafted bone approximated the cortical bone, axial loading resulted in stress reduction in all the native bone layers; however, lateral loading produced stress reduction in only the cancellous bone. When the stiffness of the graft was less than that of the cancellous bone, the graft assumed a lesser proportion of axial loads. Thus, it caused a concomitant stress increase in all the native bones, whereas this phenomenon was observed in only the cancellous bone with lateral loading. The crestal cortical bone, though receiving the highest intensity stresses, affected the overall stress distribution less than the grafted bone. The stress from the lateral load was up to 11 times higher than that of the axial load around the implant. These findings suggest that the type of loading affects the load distribution more than the variations in bone, and native bone is the primary supporting structure.

Mete I. Fanuscu, DDS, *is an assistant professor and director of Advanced Education in General Dentistry, Division of Restorative Dentistry, School of Dentistry, University of California, Los Angeles. Address correspondence to Dr Fanuscu at UCLA School of Dentistry, CHS, 20-114, 10833 Le Conte Avenue, Los Angeles, CA 90095 (e-mail: mfanuscu@ucla.edu).*

Hung V. Vu, DDS, PhD, *is a professor in the Department of Mechanical and Aerospace Engineering, California State University, Long Beach, and is a clinical assistant professor of Orthodontics, Division of Craniofacial Sciences and Therapeutics, University of Southern California, Los Angeles.*

Bernard Poncelet, MS, *is a mechanical engineer for Orthodyne Electronics, Irvine, California.*

INTRODUCTION

Maxillary sinus bone-graft augmentation has become one of the most common surgical procedures for increasing bone volume for implant placement in the posterior atrophic edentulous maxilla. Since the introduction of sinus graft technique by Boyne and James,[1] various types of graft materials, implants, and procedural modifications have been proposed to

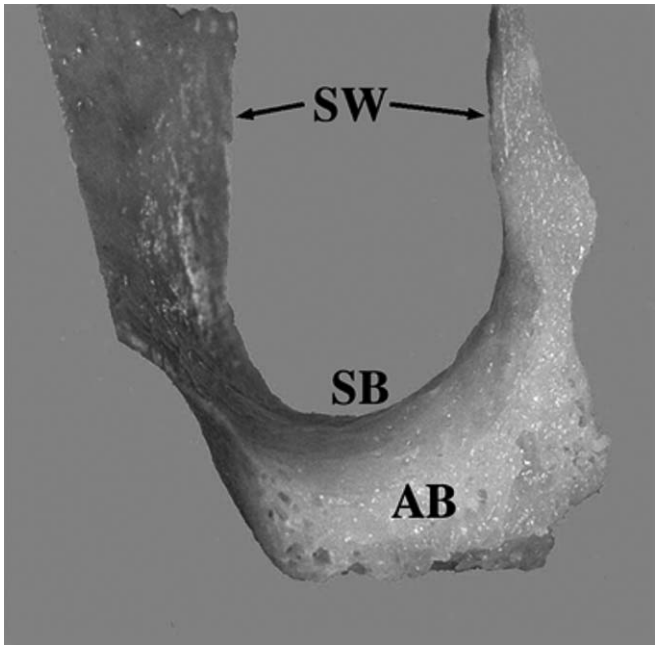

FIGURE 1. Cross section of alveolar bone (AB) with sinus base (SB) and walls (SW) in the posterior maxilla from human cadaver.

improve the efficacy of the therapy.

Bone-graft materials, such as autogenous,[2–5] allogenic,[5,6] alloplastic,[5,7] xenogenic,[5,6] and combinations of these materials[4–6,8] have been used. Sinus graft is usually considered for atrophic maxilla, such as class V and VI according to the classification of Cawood and Howell.[9] Average heights of class V and VI were reported to be 7.4 and 3.2 mm, respectively.[10] The edentulous posterior maxilla is anatomically characterized by thin cortical bone at both the crestal and sinus floor and the low-density cancellous bone (Figure 1).[11]

Depending on the preoperative bone level, simultaneous or delayed implant placement techniques have been used in sinus graft procedures. Jensen and coworkers[5] in the consensus report stated a 90% success rate for implants in sinus grafts with at least 3 years of function. The report included patients with simultaneous and delayed implant placements in various grafts. There was no indication of superiority of a particular protocol or material. However, there was a statistical difference in implant loss when available bone was 4 mm or less as opposed to 5 mm or more.

A complex structure consisting of bone with varying stiffness can be found around the implants placed in the posterior maxilla with grafted sinus. A crucial process, which leads to the stability of osseointegrated implants, is the mineralization of the bone adjacent to the implant surface. Native bone, which provides primary stability for establishing and maintaining osseointegration, consists of crestal cortical bone, cancellous bone, and sinus floor cortical bone. The contribution of the grafted bone in establishing and maintaining implant stability is not yet well known. Load-bearing characteristics of grafted bone depend on the graft material and its maturation process.[12] Several studies investigated the total volume of hard tissue within various sinus grafted tissues to predict long-term implant stability.

According to histological analysis, vital mineralized tissue volume of the grafted sinus ranged from 26% to 69% when only autogenous bone was used.[13–16] The range of vital mineralized tissue volume was 5% to 45% when any other graft material and the combinations of materials were used.[8,13,17–19] It also should be noted that the mineralized tissue volume of grafted sinus has been reported as relatively greater compared with that of native cancellous bone in the edentulous posterior maxilla, ranging from 17.1% to 26.7%.[20]

Premature loading and overloading might be significant concerns in sinus graft cases because different graft materials and their maturation patterns can have variable load-bearing capacities. Biomechanically, control of load transfer to bone surrounding the implants may play an important role for long-term success of implant therapy.[21] Several studies reported that appropriately controlled loads can stimulate bone remodeling around the implants,[22,23] whereas excessive stresses cause marginal bone resorption.[24–26] Load transfer from implants to surrounding bone depends on the type of loading, the bone-implant interface, the length and diameter of the implants, the shape and characteristics of the implant surface, the prosthesis type, and the quantity and quality of the surrounding bone.[27] Some of these biomechanical factors are inherent with the patients, and the others can be controlled by the clinicians. The effects of these factors are not well understood in grafted sinus sites, with the obvious exception that the overloading leads to failure.

Clinical studies provide important information about general trends; however, specific biomechanical variables might be more efficiently examined by using in vitro models. Accurately designed and appropriately analyzed in vitro models can be useful in studying biomechanical factors and their relations. Finite element method, a numerical modeling system, is routinely used in modern engineering practice to study complex structures and has been long used in implant-dentistry research.[28]

The purpose of this study was to investigate the stress distribution in the bone surrounding an implant placed in a posterior edentulous maxilla with sinus graft by using finite element analysis.

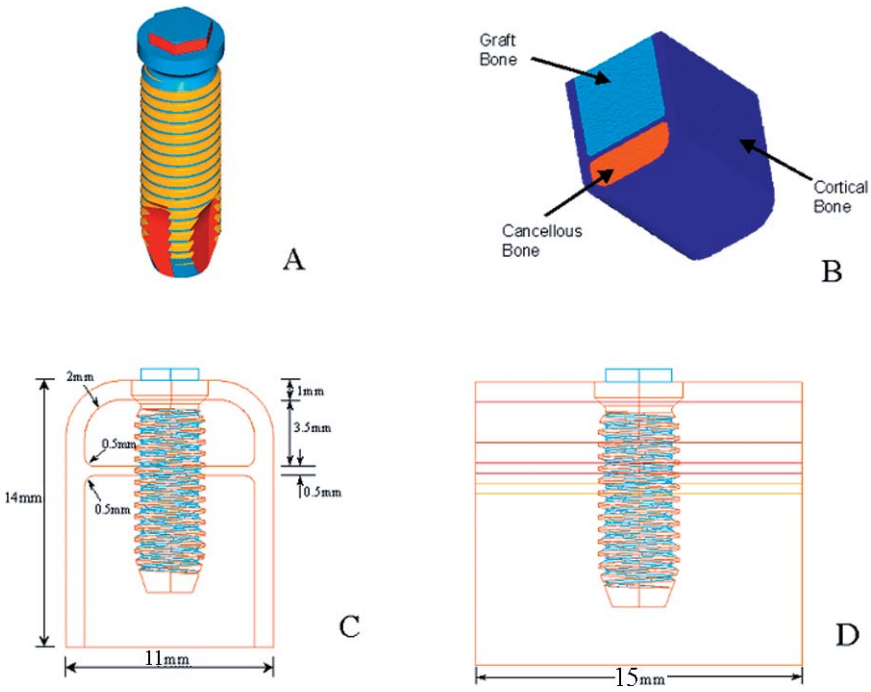

FIGURE 2. (A) Self-tapping implant, isometric view. (B) Posterior maxilla model. (C) Implant inserted, front view. (D) Implant inserted, side view.

MATERIALS AND METHODS

The software I-DEAS 9 (SDRC Inc, Cincinnati, Ohio) was used for preprocessing, finite element analysis, and postprocessing in the study. It not only was convenient to use the same software package for both the design and the analysis, but it also avoided potential compatibility errors among different programs.

The predictive accuracy of a mechanical finite element model is influenced by 4 parameters: geometric detail, element type and count, material properties, and applied boundary conditions.[29] The parameters were carefully taken into consideration in the present study.

Geometric detail

A 3-dimensional (3-D) model of a standard threaded implant was generated from its original mechanical drawing (ST311, Implant Innovations Inc, Palm Beach Gardens, Fla). The implant had a major diameter of 3.75 mm, a pitch of 6 mm, and a total length of 11.5 mm. High-fidelity modeling was achieved by replicating the geometry and the helical threads of the implant (Figure 2A).

A 3-D model of a unilateral edentulous posterior maxilla with grafted sinus was designed for testing and analysis. The model consisted of 1-mm crestal cortical, 3.5-mm cancellous, 0.5-mm sinus cortical, and 9-mm grafted bone components (Figure 2B, C, and D). The total height of the native bone components was 5 mm throughout the study; however, the thickness of the crestal cortical bone was changed from 1 mm to 0.2 mm to test anatomical variance, where cancellous bone thickness was increased accordingly. The graft placement was considered to be complete peri-implant packing as suggested by Tepper et al[30] and to be an ideal case.

The model was assumed to have 100% union between the grafted maxillary bone and the implant, representing ideal osseointegration. Mesial and distal views of the model were symmetrical as were the buccal and palatal views.

Element type and count

Parabolic tetrahedral elements were used. A first mesh was generated and then fine tuned by redefining the number of elements on certain edges of interest and by changing the element size and the maximum percentage of curvature deviation allowed. This was accomplished by using the automatic remeshing tool included in I-DEAS that refines the original mesh, based on the stress-energy results obtained from the first analysis. The final mesh resulted in 22 614 elements and 32 453 nodes.

Material properties

The properties of the materials used in the study are listed in

TABLE 1
Materials' properties for implant and tissues

	Elastic Modulus (GPa)	Poisson's Ratio
Titanium[31]	103.4	0.35
Cortical[32]	14.0	0.30
Cancellous[32]	1.4	0.30
Graft (stiff)	11.0	0.30
Graft (less stiff)	0.5	0.30

Table 1. All the values for the modulus of elasticity and Poisson's ratio remained constant throughout the testing, except for the grafted bone, which was proposed to represent the upper and lower range of stiffness. All the materials used in this model were assumed to be isotropic, homogenous, and linearly elastic.

Applied boundary conditions

Boundary conditions of the model were defined with zero displacement of translation and rotation on both mesial and distal surfaces of the bone complex.

Two different cases of loading were simulated: (1) Axial loading: A force of 300 N was applied at the center of the top surface of the implant and in the long-axis direction (Figure 3A). (2) Lateral loading: A force of 300 N was applied at a point 5 mm away from the center top surface of the implant, perpendicular to the long axis, and in the buccal-palatal direction (Figure 3B). This would be for the lateral load on the crown; direct application of the load was not possible because the model did not include the crown. Thus, an equivalent system of a lateral force of 300 N and a coupled moment (5 mm $\times$ 300 N) was used. For simulation in I-DEAS, the lateral force of 300 N was modeled as 4 lateral forces of 75 N (4 $\times$ 75 N = 300 N). The coupled moment of 5 mm $\times$ 300 N was modeled as a set of 2 parallel forces of 491 N separated by 3.048 mm (3.048 mm $\times$ 491 N = 5 mm $\times$ 300 N). These 2 parallel forces were in the long-axis direction.

The variation in the graft quality and crestal cortical anatomy produced the following 4 clinical scenarios to be modeled:

- Strong graft with thick crest (STk): stiff grafted bone and thick crestal cortical bone
- Weak graft with thick crest (WTk): less-stiff grafted bone and thick crestal cortical bone
- Strong graft with thin crest (STn): stiff grafted bone and thin crestal cortical bone
- Weak graft with thin crest (WTn): less-stiff grafted bone and thin crestal cortical bone

RESULTS

A 3-D finite element (3D-FE) model was used to study implant biomechanics in grafted sinus. Models STk, WTk, STn, and WTn were analyzed when axial and lateral loads were applied. The results indicated 3 global stress patterns: (1) stress was highest within the cortical bones, lower within the grafted bone, and lowest within the cancellous bone; (2) stresses produced with off-axial loads were higher in the cortical and grafted bones and lower in the cancellous bone compared with axial loads; and (3) high stress concentrations were evident at the helical threads.

Axial loading

Figure 4 shows the von Mises stress distribution in the simulated bone components in all 4 models under axial loading. The stresses were higher in the crestal cortical bone when compared with sinus floor cortical bone. The highest stress within the sinus floor cortical bone was found where the implant thread entered that layer. The stresses in the cancellous bone were at least 10 times less than the crestal cortical bone. However, a specific stress concentration was noteworthy at the bottom of the cancellous layer where a small portion was wedged between the thread of the implant and the sinus floor cortical bone. Regarding the grafted bone, the stress was highest at the first thread and decreased with the subsequent threads.

Comparative analysis of the stress distribution patterns in models STk, WTk, STn, and WTn suggested that stiffness of the graft was the determining factor in axial loading. When the crestal cortical was thick in models STk and WTk but model WTk had less-stiff graft, a 2- to 3-fold increase in the stress was evident in the native bone components of model WTk with concomitant decrease in the grafted bone. Models STk and STn produced similar stress distribution patterns, indicating minimal influence from the thickness of crestal cortical bone when the graft was stiffer in both models. When the models STk and WTn were compared, stress increase in the native bone and concomitant decrease in the grafted bone were noted. The presence of stiffer graft influenced the comparison between models WTk and STn in the same way it did between STk and WTk. It was interesting to note that when there was a 5-fold difference in the thickness of crestal cortical bone between models with less-stiff graft (WTk

and WTn), there was only a 20% stress increase in the native bone components in WTn. Comparing the thin crestal cortical models of STn and WTn was similar to the comparison of STk and WTk, because increased stress in the native bone and decreased stress in the grafted bone were observed in model WTn with less-stiff graft.

Lateral loading

Figure 5 shows the von Mises stress distribution in the simulated bone components in all 4 scenarios under lateral loading. The stress in the individual bone from the lateral load was up to 11 times higher than that of the axial load in the area surrounding the implant. The stress distribution in the models with stiffer graft was characterized by high stresses that were compressive on the load-applied side and tensile on the other side. It was also noted in these models that stress decreased rapidly as the depth increased both within each bone layer and along the implant. There was 8-fold less stress in the stiff grafted bone compared with the crestal cortical bone, even though they had similar modulus of elasticity and this variation widened significantly, up to 80-fold, with less-stiff graft models. The intensity of the stresses increased in the native bone, as the pattern of compressive on the load-applied side and tensile on the other side remained the same in the models with less-stiff graft. However, the stress distribution pattern was different in the less-stiff grafted bone, as evidenced by the stress concentration around the apical portion of the implant.

Comparative analysis of the stress distribution patterns in the studied models suggested that the lateral loading produced significant stress concentrations in the upper portion of the implant, affecting the native bone and thus reducing the contribution of the stiffer graft. The presence of less-stiff graft in model WTk caused no change in the cortical bone, 1-fold stress increase in the cancellous bone, and 9-fold stress decrease in the grafted bone when models of thick crestal cortical bone, STk, and WTk were compared. The model STn with thin crestal cortical bone had relative stress increases of 50% in cortical bone, 5-fold increase in the cancellous bone, and 2-fold increase in the grafted bone when the graft was stiffer in both STk and STn. Model WTn with less-stiff graft and thin crestal cortical showed 50% stress increase in the cortical bone, 8-fold increase in

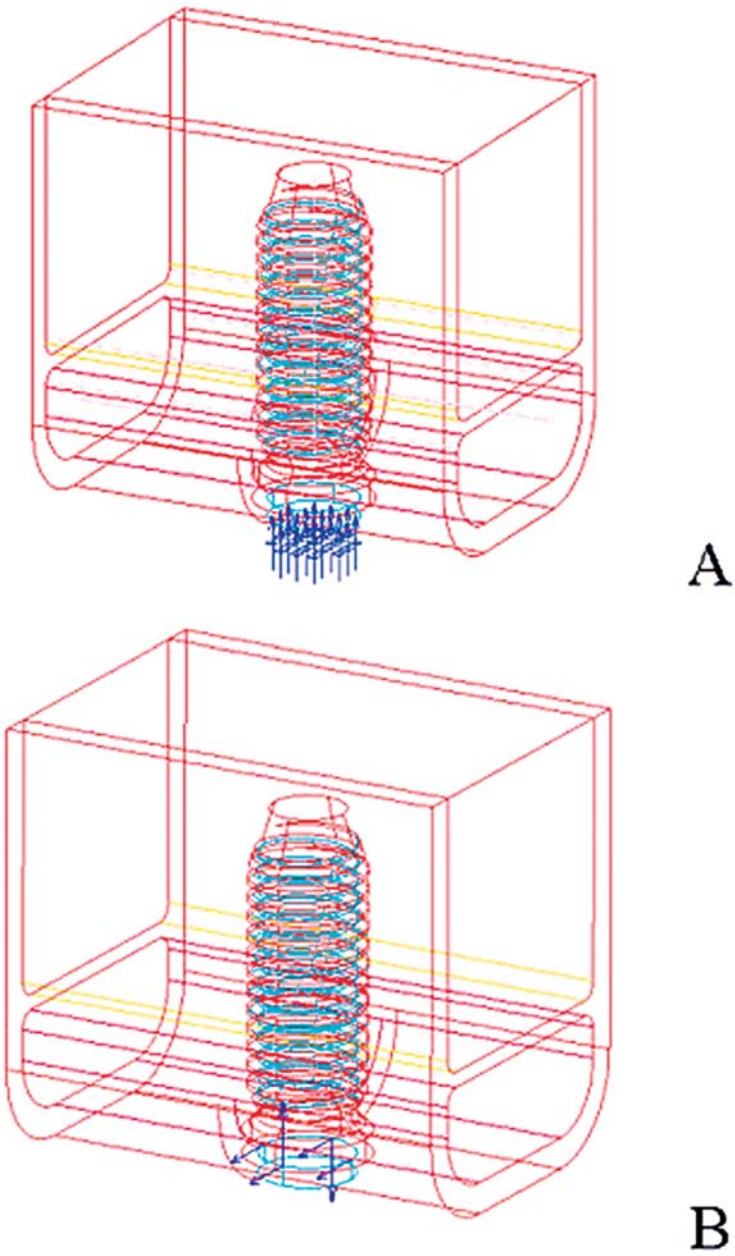

FIGURE 3. 300 N equivalent force and moment. (A) Axial loading. (B) Lateral loading.

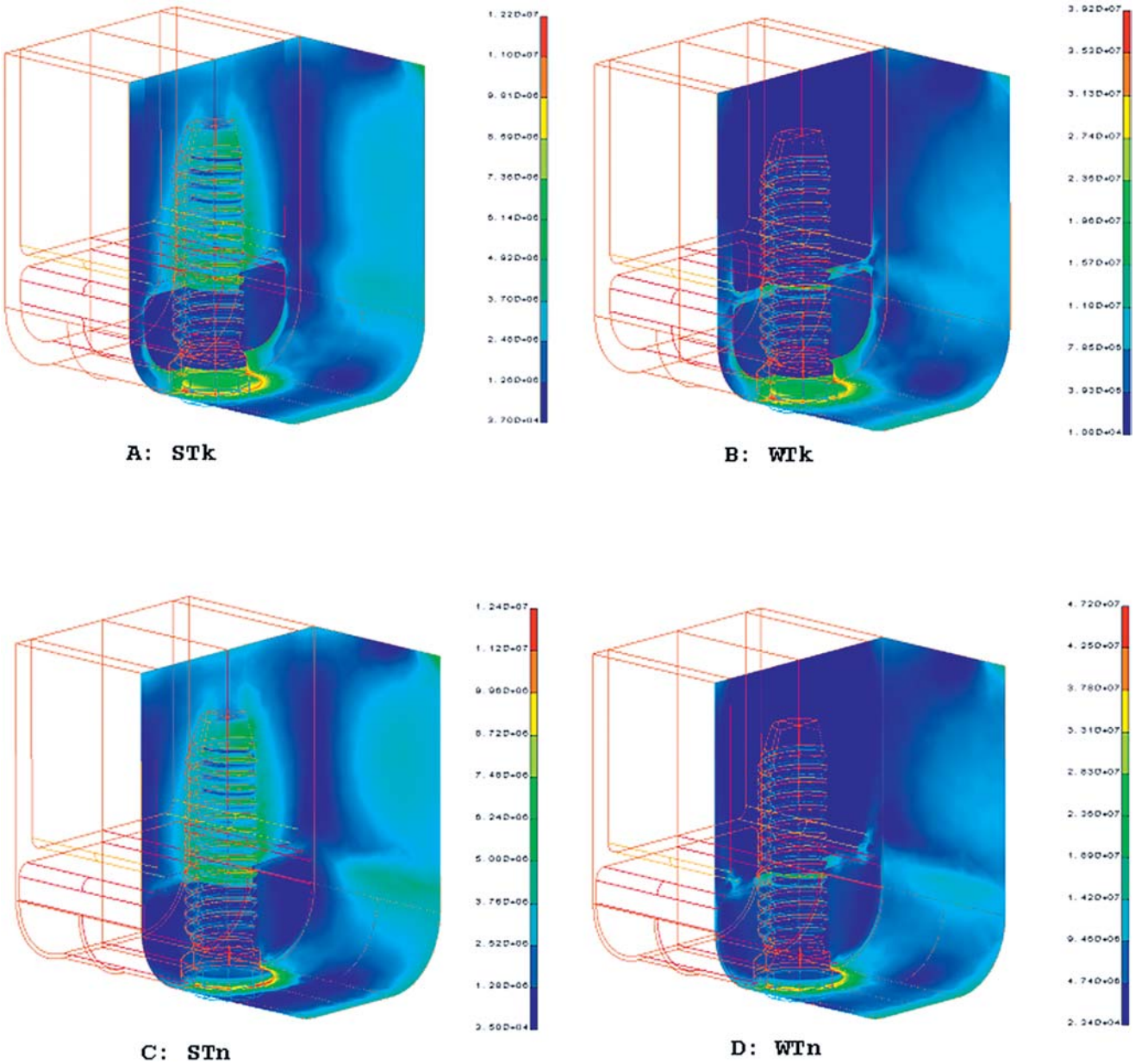

FIGURE 4. von Mises stress (N/mm^2) distribution for axial loading. (A) Strong graft with thick crest. (B) Weak graft with thick crest. (C) Strong graft with thin crest. (D) Weak graft with thin crest.

the cancellous bone, and 4-fold decrease in the grafted bone when compared with model STk. Compared with model WTk, model STn demonstrated 50% higher stresses in the native bones and 16-fold higher stresses in the grafted bone. With graft being less stiff in models WTk and WTn, thin crestal cortical bone in model WTn caused approximately half-fold increased stress in cortical bones, 4-fold increase in cancellous bone, and 1-fold increase in grafted bone. When crestal cortical bone was thin in both models STn and WTn, the model with less-stiff graft (WTn) did not yield any differences in stresses in cortical bones; however, a 65% increase in cancellous bone and a 10-fold decrease in grafted bone were observed.

DISCUSSION

A dimensionally similar model of a posterior maxilla with grafted sinus was designed by using variations in graft quality and anatomy to represent different clinical cases. High and low values

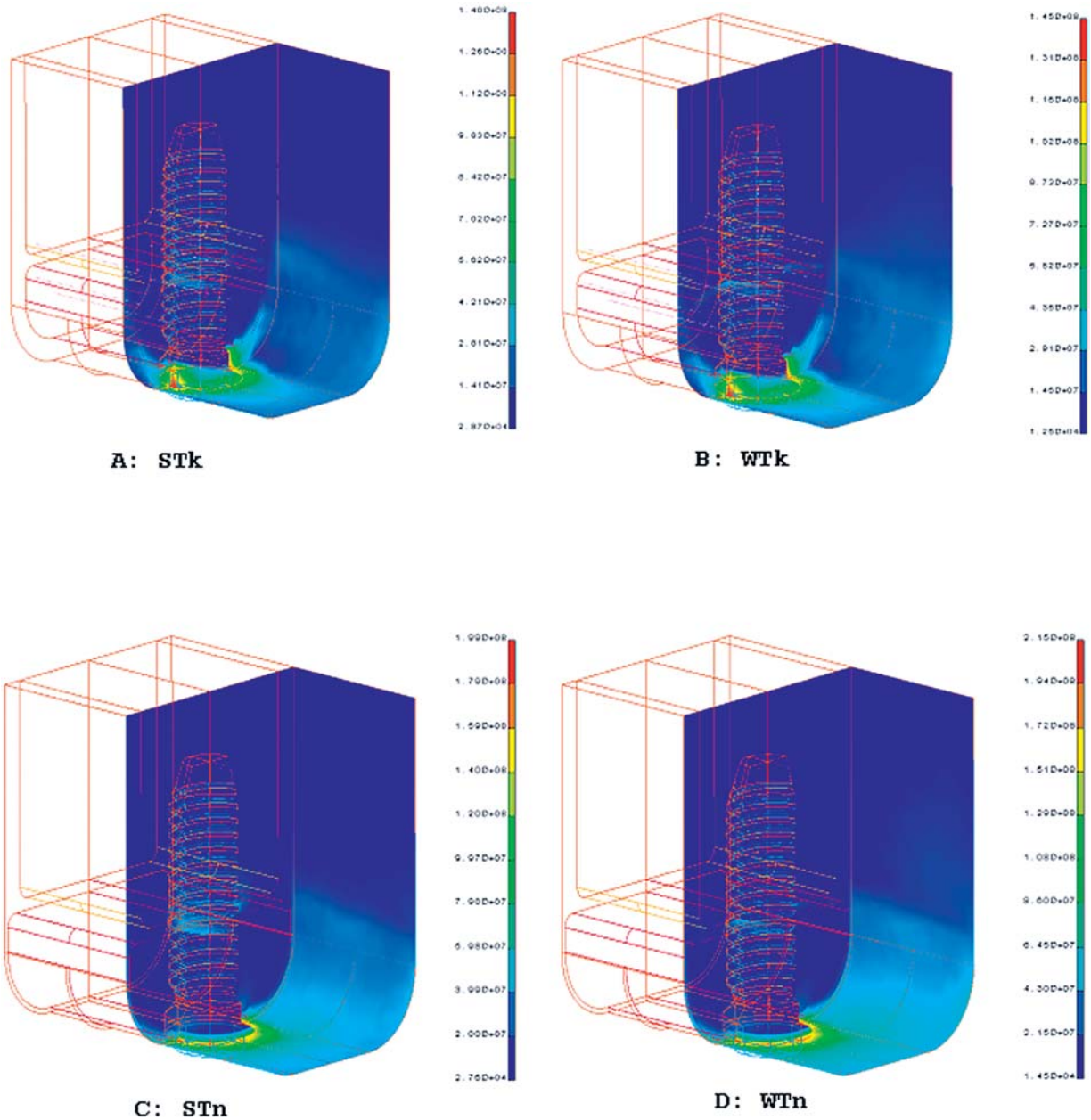

FIGURE 5. von Mises stress (N/mm^2) distribution for lateral loading. (A) Strong graft with thick crest. (B) Weak graft with thick crest. (C) Strong graft with thin crest. (D) Weak graft with thin crest.

within each variation were assigned to cover a wide range of possible scenarios. The presence of either 0.2- or 1.0-mm thick crestal cortical bone was basically a clinical correlation to minimal cortical bone or nominal cortical bone for this anatomy. The elastic modulus values for alveolar and grafted bones are not well known; however, substantial differences in stiffness have been indicated among them (Table 1). Approximately 10-fold difference in Young's modulus between cortical and cancellous bones seems to exist in the literature.[32] However, bone graft in the sinus might have a range of Young's modulus values depending on the choice of graft materials and maturation. Because assigning the elasticity value in the finite element model has a direct impact over the analysis, a high value approximating cortical bone stiffness and a low value below the stiffness of cancellous bone were used to represent a wide spectrum for achieving predictive accuracy in bone-graft modeling.

Finite element analysis can provide insight to the complex

mechanical behavior of natural and restored craniofacial structures affected by 3-D stress fields, which are still very difficult to assess otherwise. Even though the distribution of forces in peri-implant bone has been investigated by finite element analysis in several studies,[33,34] a comparison of 2-dimensional finite element analyses and 3D-FE analyses in one study showed that only 3D-FE analysis could realistically simulate the stress pattern in space.[35] Finite element modeling, like all in vitro studies that use model systems, has advantages and limitations. The 3-D model in this study was designed with precise geometry of the implant and the anatomy along with appropriate element type and count; however, certain assumptions were made in material properties and applied boundary conditions because of a lack of data and technology. Besides, technical difficulty in adjusting the degree of osseointegration led to the assumption of 100% osseointegration in the study. Few studies were carried out on bone-implant contact with retrieved titanium microimplants from human posterior maxilla with grafted sinus.[12,36] They revealed less bone-implant contact area in the grafted-bone portion, particularly for implants placed simultaneous with bone graft, than that in the native bone portion. Although there is no evidence of relationship between degree of bone-implant contact and stress distribution, potentially much higher magnitudes of stress might concentrate in the native bone-implant interface when the interface of the implant with grafted bone is diminished. In the finite element model, because of the complete osseointegration in both native and grafted bone, the magnitude of stresses might be different than the clinical situation. However, the trends of stress distribution would not be substantially changed in the comparison of different situations. These trends were effectively demonstrated in the complex model under axial and off-axial loads. The mechanical behavior observed in this study was also validated in a previous study by one of the authors where photoelastic modeling with similar geometry was used.[37]

The 3D-FE model in the present study yielded results in agreement with previous investigations in terms of occurrence of greatest stresses in the crestal cortical bone and stress magnification with off-axial loading.[34,38] A recent 3D-FE study of sinus grafted posterior maxilla, where quality of sinus graft simulated in that study would correspond to poor-quality graft case in our study, also demonstrated similar stress distribution patterns in which higher-level stresses were localized at the crestal and sinus cortical bones as well as around the implant apex.[30]

The results for axial loading indicate that some portions of the high-level stresses from the native bone might be transferred to the grafted bone along the implant depending on the quality or maturity of grafted bone in sinus. Therefore, the high reliance on the native bone can be reduced by altering the load distribution pattern with high-quality or mature grafted bone. However, the variation in the native bone anatomy might have a mild effect in the overall pattern of high crestal stresses. Having higher stresses around the upper portion of the implant when minimal cortical bone exists might challenge the load-bearing capacity of native bone, especially in cases of poor-quality grafted bone. Several in vivo studies demonstrated that excessive marginal bone loss in the cortical bone around implants was associated with occlusal overloads.[21–23]

The resorptive pattern of alveolar bone in the maxilla usually leads to the palatal placement of the implants, which, in turn, yields buccally cantilevering restorations. The application of the lateral loads represented this phenomenon in the present study. The lateral loads affected not only the localization of stresses but the magnitude as well. Highest overall stresses were noted in the cortical bones under lateral loads, whereas cancellous bone received lowest overall stresses. The 2 layers of cortical bone seemed to play the most critical role in supporting the implant in this anatomy, because high-quality graft decreased stresses in only the cancellous bone. Therefore, the quality of a graft is of particular concern when the amount of existing cancellous bone is limited, as this would intensify the stresses in the cancellous bone. This may explain the decreased success rates when implants are placed in posterior sites with less than 5 mm of bone in combination with sinus grafts.[5]

The 3-D model of the implant in the present study took into account the phenomena created by the helical nature of the thread that has never been modeled as precisely before. Stress concentrations at the tip of the threads were observed along the implant; however, some exceptional stress concentrations were also noted at the transitional areas of the multi-layered bone as the thread entered and exited bone layers. This was because of the less-stiff bone being compressed between implant and stiff bone. This might be of interest in designing implants for this anatomy in the future.

This in vitro biomechanical

study suggests that loading pattern, amount of native bone, and quality of sinus graft might have a descending order of importance in the equitable load distribution at the posterior maxilla.

Acknowledgments

The authors would like to thank Dr Russell D. Nishimura of UCLA School of Dentistry for giving advice in preparation of the manuscript. This study was presented in part at the American Academy of Implant Dentistry Annual Meeting, October 2002, Los Angeles, Calif, and was partially supported with a grant awarded by American Academy of Implant Dentistry Research Foundation in 2000.

References

1. Boyne PJ, James RA. Grafting of maxillary sinus floor with autogenous marrow and bone. *J Oral Surg.* 1980;38:613–618.

2. Kent JN, Block MS. Simultaneous maxillary sinus floor bone grafting and placement of hydroxyapatite-coated implants. *J Oral Maxillofac Surg.* 1989;47: 238–242.

3. Blomqvist JE, Alberius P, Isaksson S. Two-stage sinus reconstruction with endosseous implants: a prospective study. *Int J Oral Maxillofac Implants.* 1998;13: 758–766.

4. Watzek G, Weber R, Bernhart T, Ulm C, Haas R. Treatment of patients with extreme maxillary atrophy using sinus floor augmentation and implants: preliminary results. *Int J Oral Maxillofac Surg.* 1998;27:428–434.

5. Jensen OT, Shulman LB, Block MS, Iacono VJ. Report of the sinus consensus conference of 1996. *Int J Oral Maxillofac Implants.* 1998;13(suppl):758–766.

6. Fugazzotto PA, Vlassis J. Long-term success of sinus augmentation using various surgical approaches and grafting materials. *Int J Oral Maxillofac Implants.* 1998;13:52–58.

7. Wheeler SL, Holmes RE, Calhoun CJ. Six-year clinical and histologic study of sinus–lift grafts. *Int J Oral Maxillofac Implants.* 1996;11:26–34.

8. Valentini P, Abensur D. Maxillary sinus floor elevation for implant placement with demineralized freeze-dried bone and bovine bone (Bio-Oss): a clinical study of 20 patients. *Int J Periodont Restor Dent.* 1997;17: 233–241.

9. Cawood JI, Howell RA. A classification of the edentulous jaws. *Int J Oral Maxillofac Surg.* 1988;17:232–236.

10. Ulm CW, Solar P, Gsellmann B, Matejka M, Watzek G. The edentulous maxillary alveolar process in the region of the maxillary sinus: a study of physiological dimensions. *Int J Oral Maxillofac Surg.* 1995;24: 279–282.

11. Friberg B, Sennerby L, Roos J, Lekholm U. Identification of bone quality in conjunction with insertion of titanium implants. *Clin Oral Implant Res.* 1995;6:213–219.

12. Jensen OT, Sennerby L. Histologic analysis of clinically retrieved titanium microimplants placed in conjunction with maxillary sinus floor augmentation. *Int J Oral Maxillofac Implants.* 1998;13:513–521.

13. Moy PK, Lundgren S, Holmes R. Maxillary sinus augmentation: histomorphometric analysis of graft materials for maxillary sinus floor augmentation. *J Oral Maxillofac Surg.* 1993; 51:857–862.

14. Lundgren S, Moy PK, Johansson C, Nilsson H. Augmentation of the maxillary sinus floor with particulated mandible: a histologic and histomorphometric study. *Int J Oral Maxillofac Implants.* 1996;11:760–766.

15. Blomqvist JE, Alberius P, Isaksson S, Linde A, Obrant K. Importance of bone graft quality for implant integration after maxillary sinus reconstruction. *Oral Surg Oral Med Oral Pathol Oral Radiol Endod.* 1998;86:268–274.

16. Lorenzetti M, Mozzati M, Campanino PP, Valente G. Bone augmentation of the inferior floor of the maxillary sinus with autogenous bone or composite bone grafts: a histologic-histomorphometric preliminary report. *Int J Oral Maxillofac Implants.* 1998; 13:69–76.

17. Wheeler SL. Sinus augmentation for dental implants: the use of alloplastic materials. *J Oral Maxillofac Surg.* 1997;55: 1287–1293.

18. Hanisch O, Lozada JL, Holmes RE, Calhoun CJ, Kan JYK, Spiekermann H. Maxillary sinus augmentation prior to placement of endosseous implants: a histomorphometric analysis. *Int J Oral Maxillofac Implants.* 1999;14: 329–336.

19. Froum SJ, Tarnow DP, Wallace SS, Rohrer MD, Cho SC. Sinus floor elevation using anorganic bovine bone matrix (osteograf/n) with and without autogenous bone: a clinical histologic, radiographic, and histomorphometric analysis—part 2 of an ongoing prospective study. *Int J Periodont Restor Dent.* 1998; 18:529–543.

20. Watzek G, Ulm CW, Haas R. Anatomic and physiologic fundamentals of sinus floor augmentation. In: Jensen OT, ed. *The Sinus Bone Graft.* Chicago, Ill: Quintessence; 1999: 31–47.

21. Esposito M, Hirsch JM, Lekholm U, Thomsen P. Biological factors contributing to failures

of osseointegrated oral implants (II). Etiopathogenesis. *Eur J Oral Sci.* 1998;106:721–764.

22. Adell R, Lekholm U, Rockler B, et al. Marginal tissue reactions at osseointegrated titanium fixtures (I). A 3-year longitudinal prospective study. *Int J Oral Maxillofac Surg.* 1986;15: 39–52.

23. Sennerby L, Lundgren S. Histologic aspects of simultaneous implant and graft placement. In: Jensen OT, ed. *The Sinus Bone Graft.* Chicago, Ill: Quintessence; 1999:95–105.

24. Lindquist LW, Rockler B, Carlsson GE. Bone resorption around fixtures in edentulous patients treated with mandibular fixed tissue-integrated prostheses. *J Prosthet Dent.* 1988;59: 59–63.

25. Quirynen M, Naert I, van Steenberghe D. Fixture design and overload influence marginal bone loss and fixture success in the Branemark system. *Clin Oral Implant Res.* 1992;3:104–111.

26. Isidor F. Loss of osseointegration caused by occlusal load of oral implants. *Clin Oral Implant Res.* 1996;7:143–152.

27. Rangert B, Sennerby L, Nilson H. Load factor analysis for implants in the resorbed posterior maxilla. In: Jensen OT, ed. *The Sinus Bone Graft.* Chicago, Ill: Quintessence; 1999:167–176.

28. Geng J-P, Tan KBC, Liu G-R. Application of finite element analysis in implant dentistry: a review of the literature. *J Prosthet Dent.* 2001;85:585–598.

29. Korioth TWP, Verslus A. Modeling the mechanical behavior of the jaws and their related structures by finite element analysis. *Crit Rev Oral Biol Med.* 1997;8:90–104.

30. Tepper G, Haas R, Zechner W, Krach W, Watzek G. Three-dimensional finite element analysis of implant stability in the atrophic posterior maxilla. *Clin Oral Implant Res.* 2002;13:657–665.

31. del Valle V, Faulkner G, Wolfaardt J, Dent M. Craniofacial osseointegrated implant-induced strain distribution: a numerical study. *Int J Oral Maxillofac Implants.* 1997;12:200–210.

32. Spector M. Basic principles of tissue engineering. In: Lynch SE, Genco RJ, Marx RE, eds. *Tissue Engineering: Applications in Maxillofacial Surgery and Periodontics.* Chicago, Ill: Quintessence; 1999:3–16.

33. Rieger MR, Fareed K, Adams WK, Tanquist RA. Bone stress distribution for three endosseous implants. *J Prosthet Dent.* 1989;61:223–228.

34. O'Mahony A, Bowles Q, Woolsey G, Robinson SJ, Spencer P. Stress distribution in the single-unit osseointegrated dental implant: finite element analyses of axial and off-axial loading. *Implant Dent.* 2000;9:207–216.

35. Ismail YH, Pahountis LN, Fleming JF. Comparison of two-dimensional and three-dimensional finite element analysis of a blade implant. *Int J Oral Implant.* 1987;4:25–31.

36. Watzek G, Ulm CW, Haas R. Anatomic and physiologic fundamentals of sinus floor augmentation. In: Jensen OT, ed. *The Sinus Bone Graft.* Chicago, Ill: Quintessence; 1999:31–47.

37. Fanuscu MI, Iida K, Caputo AA, Nishimura R. Load transfer by an implant in sinus grafted maxillary model. *Int J Oral Maxillofac Implants.* 2003; 18:667–674.

38. Borchers L, Reichart P. Three-dimensional stress distribution around a dental implant at different stages of interface development. *J Dent Res.* 1983;62: 155–159.